AUT Journal of Electrical Engineering
10.22060/EEJ.2026.25791.6005

Designing a robust method to improve voltage control of DC-DC buck converters

Farhad Amiri[1*], Sajad Sadr[2]

1 Department of Electrical Engineering, Tafresh University, Tafresh, Iran, f.amiri@tafreshu.ac.ir

2 Department of Electrical Engineering, Tafresh University, Tafresh, Iran, sadr@tafreshu.ac.ir

* Correspondence: f.amiri@tafreshu.ac.ir

Abstract: Given that the DC-DC buck converter (DDBC) is an example of a nonlinear system, and also considering the disturbance and changes related to its parameters, the output voltage control in this DDBC will face several challenges. In this paper, a PD-PI cascaded controller is designed to control the voltage in the DC-DC buck converter. In this cascaded controller, the PD controller, as the outer loop controller, is responsible for responding quickly to voltage changes and damping them, and the PI controller is responsible for eliminating the error caused by voltage changes. Considering that the accurate and optimal adjustment of the parameters related to the cascaded controller is crucial to its performance, the Grey Wolf Optimizer algorithm has been employed to optimize these parameters. This algorithm offers several advantages, including intelligent search, parameter fine-tuning, and stable and rapid convergence. To assess the robustness of the proposed PD-PI(Grey Wolf Optimizer) approach against disturbances and parameter variations, multiple scenarios were developed and its performance compared with that of control strategies like PD-PI (Electric Eel Foraging Optimizer) and PD-PI (Flood algorithm). According to the results, the proposed method outperforms other control methods in terms of various criteria, including Settling time, Rise time, Peak time, Overshoot, and Steady state error.

Keywords: DC-DC buck converters**,** output voltage control, cascaded controller, Performance Improvement

AUT Journal of Electrical Engineering
10.22060/EEJ.2026.25791.6005

Abbreviations:

GWO	Grey Wolf Optimizer
PD	proportional (P) derivative(D)
PI	Proportional integral
EEFO	Electric Eel Foraging Optimizer
FLA	Flood algorithm
ST	Settling time
t_{rise}	Rise time
t_{peak}	Peak time
Os	Overshoot
e_{ss}	Steady state error
GA	Genetic algorithm
WOA	whale optimization algorithm
EA	evolutionary algorithms
SOA	snake optimization algorithm
FDBRUN	Fitness-Distance Balance Based Runge Kutta
MPC	Model predictive control
SMC	Sliding mode *controller*
HKMG	Hybrid k-means Grasshopper Optimization Algorithm
ISE	Integral of squared error
ITSE	Integral of time multiplied by squared error
IAE	Integral of absolute error
ITAE	Integral of time multiplied by absolute error
FOPID	Fractional order proportional - integral -derivative

1-Introduction:

In the modern electrical industry, the proliferation of diverse consumer applications has necessitated a wide spectrum of operating voltage levels [1]. These requirements range from a fraction of a volt to several volts, depending on the specific demands of power supplies, electric motor starters, and various household appliances [2]. To provide these regulated voltage levels from a single source, DC-DC converters have become indispensable components [3]. Generally, these converters are classified into three primary topologies: buck converters for step-down applications, boost converters for step-up operations, and buck-boost converters, which offer the flexibility to either increase or decrease the input voltage [4]. Among these, the Buck DC-DC Converter (DDBC) is widely utilized for stepping down high DC voltages to lower, regulated levels with efficiencies often exceeding 90% [5]. The DDBC is highly valued in practical electrical applications due to its high response speed to load changes, precise output voltage regulation, and effective filtering of unwanted fluctuations, all of which contribute to minimized energy loss and reduced heat generation [6]. The DDBC is a nonlinear system characterized by complex dynamics in capacitor voltage and inductor current, arising from the MOSFET-driven switching mechanism [7]. If there is no controller in the DDBC, it will have poor performance against load changes, disturbances, and changes in the parameters of the related elements, such as inductors and capacitors, and will move the output voltage of DDBC away from its reference value [8-10]. Consequently, various control strategies have been implemented to regulate the DDBC voltage.

10.22060/EEJ.2026.25791.6005

These methods aim to enhance the converter's stability and dynamic response while ensuring robustness against disturbances and parameter uncertainties. Various control strategies have been explored in the literatures to regulate the output voltage of the DDBC. Early approaches primarily employed conventional PI controllers [11-13], which, despite their structural simplicity and effectiveness against slow-varying disturbances, exhibited poor robustness against sudden changes in load and input. In [14,15], a PID controller is used to control the voltage in the DDBC. This controller has a faster response than a PI controller and has a good performance against sudden changes in load and reference. However, in this method, both damping and response speed objectives cannot be improved simultaneously. In [16-18], a PID controller is used in a DDBC structure whose parameters are optimized by GA, WOA, and EA algorithms. The existence of these algorithms helps the PID controller to have a desirable optimal performance, and in this method, two objectives (improving response speed and improving damping of voltage fluctuations) can be achieved simultaneously. These methods have problems such as the presence of overshoot and large steady-state error in the voltage. In [19], the FOPID controller is used to control the voltage in the DC-DC buck converter. This controller has advantages over the PID controller, such as greater resistance to parameter changes, greater flexibility, and greater accuracy in tracking the reference voltage, but it still has a slow transient response and a large steady-state error in the output voltage of the DDBC.
In [20-22], the FOPID controller has been used in the DDBC structure, whose parameters have been optimized by the SOA, FDBRUN, and HKMG algorithms. Employing various optimization algorithms to tune the FOPID controller parameters in a DDBC enhances key performance metrics—such as settling time, steady-state error, and voltage overshoot—relative to a conventional PID controller. But it still has problems, such as computational complexity for practical design and a lack of separation of steady-state and transient tasks in the DDBC. In [23, 24], the Fuzzy-PID controller has been used for voltage control in the DDBC. This method has advantages such as inherent compatibility with the nonlinear behavior of the DC-DC buck converter, simultaneous improvement of transient and steady-state response, but it has many challenges, including: 1) complex design and adjustment, 2) implementation problems due to high computational load, and 3) possible increase in overshoot and undershoot related to output voltage fluctuations of the DDBC if not designed properly. In [25], a Fuzzy-PID controller is used for voltage control in a DDBC. In [26], neuro fuzzy control controller is used for voltage control in a DDBC. In this method, a neural network is used for data learning power and automatic adjustment of membership functions and rule parameters in the fuzzy system, and fuzzy logic is used to manage uncertainty caused by changes in parameters related to the DDBC, which will improve dynamic response, reduce overshoot, and provide better resistance to parameter changes than a fuzzy controller. But it has problems such as complexity in design, high cost for training, and difficulty in implementing in practice. It is difficult to use this method for DDBC control.

In [27, 28], the MPC controller is used to control the voltage of the DDBC. This control method improves the steady-state voltage response and reduces the overshoot related to voltage fluctuations in the DDBC, but it does not perform well against disturbances entering the DDBC. In [29, 30], the SMC controller is used to control the voltage of the DDBC. This method has good resistance to disturbances and parameter changes and provides an accurate response for the converter. However, it has several problems, including the chattering phenomenon, dependence

on uncertainty bounds, and the need for additional sensors. In [31], voltage regulation of the DDBC is achieved through a cascaded PI-PD controller, whose parameters are tuned using the EEFO algorithm. The proposed technique is benchmarked against PID, PIDA, and FOPID controllers, and its advantages over these methods are validated in terms of overshoot, settling time, rise time, and steady-state error. The method proposed in [31], in addition to the aforementioned advantages, also has some disadvantages, such as the EEFO algorithm having a slow convergence speed, and due to being trapped in a local optimum and high sensitivity to parameter settings, the performance of the PI-PD cascaded controller has faced challenges. Therefore, for voltage control in the buck converter, a robust control method is needed that is resistant to disturbances and parameter changes and improves the steady-state error, peak time, overshoot percentage, and rise time.

In this paper, a PD-PI cascaded controller is designed to control the voltage in the DDBC. In this cascaded controller, the PD controller, as the outer loop controller, is responsible for responding quickly to voltage changes and damping them, and the PI controller is responsible for eliminating the error caused by voltage changes. Given that the accurate and optimal adjustment of the parameters related to the cascaded controller is crucial to its performance, the GWO algorithm has been employed to optimize these parameters. This algorithm offers several advantages, including intelligent search, parameter fine-tuning, and stable and rapid convergence. In order to examine the performance of the proposed method (PD-PI(GWO)) against disturbances and changes in various parameters, several scenarios have been designed and compared with control methods such as PD-PI(EEFO) and PD-PI(FLA). According to the results, the proposed method has performed better than other control methods in terms of various criteria, including ST, t_{rise}, t_{peak}, Os, and e_{ss}. In general, the contributions of this paper include the following

- Presenting a PD-PI cascaded controller to improve the performance of the DC-DC buck converter in voltage control.
- Optimal adjustment of the cascaded controller parameters with the GWO algorithm.
- Evaluation of different algorithms (GWO, EEFO, FLA) to optimize the coefficients of the PD-PI cascaded controller considering the combined objective function (combination of transient and settling time).
- Testing the robustness of the proposed method (PD-PI(GWO)) against disturbances and changes in parameters related to the DDBC.
- Testing the proposed method (PD-PI(GWO)) in tracking the reference voltage related to the DDBC voltage and comparing it with other control methods.

The paper is organized as follows: Section 2 derives the mathematical model of the DDBC. Section 3 describes the proposed voltage control strategy. Simulation results are provided in Section 4, and the conclusions are discussed in Section 5

2- Mathematical model of DDBC

This section outlines the configuration of the DDBC and develops its state-space representation.

2-1- Structure of DDBC:

10.22060/EEJ.2026.25791.6005

The mathematical function of the DDBC is to reduce the DC voltage. In Figure 1, the structure of the DDBC is shown [30, 31]. According to this figure, DDBC includes an input voltage source v_g, an electronic switch (MOSFET), a diode, an inductor (L), a capacitor (C) and a resistive load (R) [31]. The electronic switch (MOSFET) will be switched on and off with a fixed frequency (f_s) and a period ($T_s = \frac{1}{f_s}$) by means of wide-bandwidth modulation (PWM). By switching on and off the electronic switch (MOSFET), the inductor current can be continuously increased or decreased, and the output voltage in the DDBC can also fluctuate. Given that this situation will occur over time for current or voltage and will make the DDBC nonlinear.

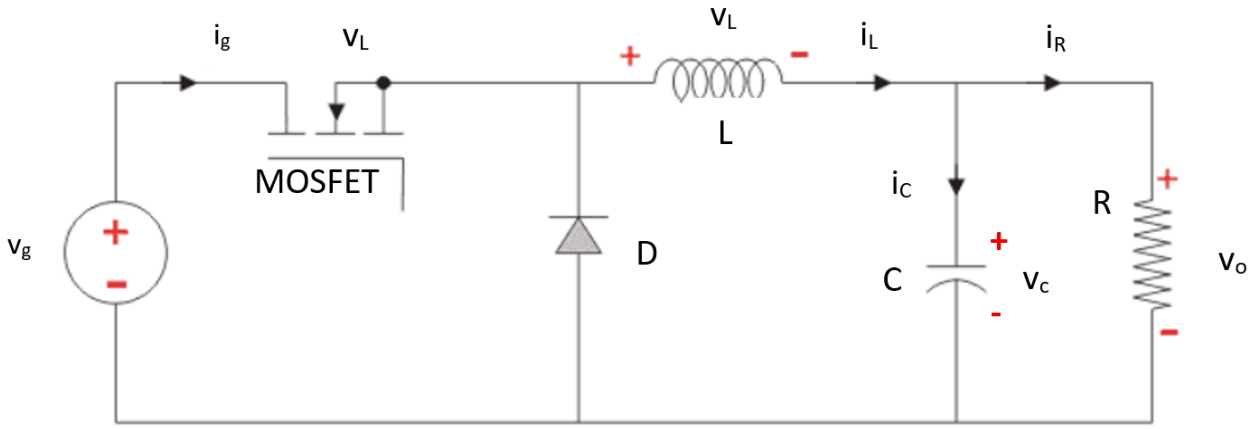

Figure 1. the structure of the DC-DC buck converter [31]

The duty cycle (D), which indicates the fraction of the total switching period that the switch is in the closed state (T_{on}), is formulated in Eq. (1) [30, 31]. Eq. (2) specifies the duration the switch remains open (T_{off}) [30, 31].

$$D = \frac{T_{on}}{T_s} \tag{1}$$

$$T_{off} = (1-D)T_s \tag{2}$$

2-2-State space model of DDBC

In DDBC, depending on the state of the switch, there will be two different circuits which will be modeled by second order state space equations. The state equations of DDBC in the switch on state ($0 \le t \le DT_s$) are shown by Eq. (3) [30].

$$\frac{d}{dt}\begin{bmatrix} i_L \\ v_o \end{bmatrix} = \begin{bmatrix} 0 & -\frac{1}{L} \\ \frac{1}{C} & -\frac{1}{RC} \end{bmatrix}\begin{bmatrix} i_L \\ v_o \end{bmatrix} + \begin{bmatrix} \frac{1}{L} \\ 0 \end{bmatrix} v_g \tag{3}$$

10.22060/EEJ.2026.25791.6005

In equation (3), v_o is the voltage across the load, i_L is the inductor current, and v_g is the input source voltage. The state equations of the DDBC in the switch-off state ($DT_s < t < T_s$) are shown by Eq. (4) [31].

$$\frac{d}{dt}\begin{bmatrix} i_L \\ v_o \end{bmatrix} = \begin{bmatrix} 0 & -\frac{1}{L} \\ \frac{1}{C} & -\frac{1}{RC} \end{bmatrix}\begin{bmatrix} i_L \\ v_o \end{bmatrix} + \begin{bmatrix} 0 \\ 0 \end{bmatrix} v_g \tag{4}$$

According to Eqs. (3) and (4), the state matrix (A) is the same in the two states of the switch being on and off, but the matrix B is different. The switching frequency in the MOSFET is much larger than the bandwidth of the control loop. Considering the weighted average of the state equations in one period with the duty cycle d and eliminating the second-order nonlinear terms, the small-signal model of the buck converter will be obtained, which will describe the dynamic behavior of small changes of the DDBC around the nominal operating point. The main transfer functions are obtained using the linearized model around the operating point according to Eqs. (5) to (8) [30, 31].

Eq. (5) presents the transfer function relating the input voltage to the output voltage.

$$G_{vg}(s) = \frac{\Delta V_0(s)}{\Delta V_g(s)} = \frac{\frac{D}{LC}}{s^2 + \frac{s}{RC} + \frac{1}{LC}} \tag{5}$$

In Eq. (5), $\Delta V_0(s)$ is the output voltage (capacitor voltage) and $\Delta V_g(s)$ is the input voltage. The transfer function of duty factor to output voltage is shown in Eq. (6).

$$G_{vd}(s) = \frac{\Delta V_0(s)}{\Delta D(s)} = \frac{\frac{V_g}{LC}}{s^2 + \frac{s}{RC} + \frac{1}{LC}} \tag{6}$$

Eq. (7) provides the transfer function that maps the input voltage to the inductor current.

$$G_{ig}(s) = \frac{\Delta I_L(s)}{\Delta V_g(s)} = \frac{\frac{D}{L}\cdot\left(s + \frac{1}{RC}\right)}{s^2 + \frac{s}{RC} + \frac{1}{LC}} \tag{7}$$

The transfer function of duty factor to inductor current is shown in Eq. (8).

10.22060/EEJ.2026.25791.6005

$$G_{id}(s)=\frac{\Delta I_L(s)}{\Delta D(s)}=\frac{\frac{V_g}{L}\cdot(s+\frac{1}{RC})}{s^2+\frac{s}{RC}+\frac{1}{LC}} \quad (8)$$

Given that in this paper, the objective is to control the output voltage in the DDBC. The objective of the proposed method (PD-PI(GWO) cascaded controller) in the DDBC structure is to change the duty cycle (D). Therefore, the transfer function from the perspective of the proposed method is according to Eq. (6) and in this case the controller will receive the voltage deviation and produce the control signal (D). The parameters related to the DDBC are shown in Table (1).

Table (1). The parameters related to the DDBC [30, 31]

parameter	value	parameter	value
v_g	36v	D	1/3
v_{ref}	12v	f_s	40000Hz
R	6Ω	T_s	$25\mu s$
L	0.001H	C	0.0001F

3- The proposed method:

In this section, the design of the proposed method (PD-PI(GWO) cascaded controller) for voltage control in the DC-DC buck converter is discussed.

3-1-PD-PI cascaded controller:

The cascaded PD-PI controller is built around a dual-loop architecture, consisting of an outer loop and an inner loop [32, 33]. This configuration endows it with several advantages over conventional single-loop controllers:

1) Separation of duties: The PD controller is used as the outer loop in the PD-PI cascaded controller. The task of this controller is to respond quickly to voltage fluctuations and damp these fluctuations. Also, in this cascaded controller, the task of the PI controller is to eliminate the steady-state error caused by voltage fluctuations. The separation of duties by the PD-PI cascaded controller will simultaneously improve the transient response and steady-state response of the voltage in the DDBC.

2) Faster response and less overshoot: Given that the derivative (D) of the PD controller is present at the beginning of the path, the damping speed of voltage fluctuations will be high, and the overshoot will have its lowest value.

3) Steady-state error close to zero: The steady-state deviation error related to the voltage in the DDBC will be close to zero by the operation of the PI controller.

4) Higher degree of freedom and more flexibility: Due to this, in the PD-PI cascaded controller

structure, there are four parameters (K_P, K_D, K_{P1}, K_I) that can be adjusted; this feature helps to shape the accurate response of the DDBC.

The transfer function of the PD controller is shown as Eq. (9) [32, 33].

$$G_{PD}(s) = K_P + K_D s \tag{9}$$

Eq. (9) incorporates a proportional gain (K_P) along with a derivative gain (K_D). The proportional gain (K_P) is used to respond quickly to voltage fluctuations and changes, and the derivative gain (K_D) is used to predict the trend of error changes and damp the fluctuations. The PI controller transfer function is shown in Eq. (10) [32, 33].

$$G_{PI}(s) = K_{P1} + \frac{K_I}{s} \tag{10}$$

In Eq. (10), a proportional gain (K_{P1}) and an integrator gain (K_I) are used. After receiving the conditioned signal from the PD controller, the proportional gain K_{P1} applies an appropriate amplification to enhance the tracking accuracy of the reference voltage, while the integral gain K_I eliminates the steady-state voltage error of the DDBC by accumulating the error over time. The architecture of the cascaded PD-PI controller is illustrated in Figure 2.

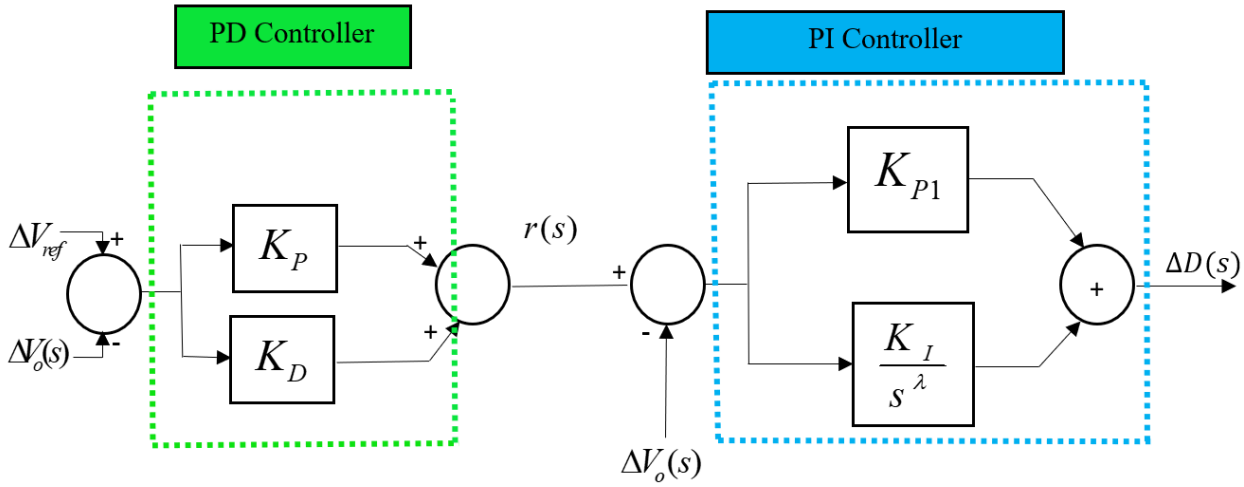

Figure 2. The architecture of the cascaded PD-PI controller

In order to ensure the effective and robust operation of the PD-PI cascaded controller against disturbances and changes in the parameters of the DDBC, the GWO algorithm has been used. The GWO algorithm has the capability of intelligent search and stable convergence.

3-2-GWO:

The gray wolf algorithm is a nature-inspired metaheuristic that models the social hierarchy and hunting strategy of gray wolves [34-36]. Due to its high convergence speed, simplicity, and high efficiency, this algorithm has been used in this paper to adjust the PD-PI controller parameters in the DDBC structure. In this algorithm, gray wolves are divided into four different categories: 1)

10.22060/EEJ.2026.25791.6005

Wolf α (alpha group leader), 2) Wolf β (helper to the group leader), 3) δ: middle members of the group, 4) ω: low-ranking members.

According to this algorithm, the top three wolves (α, β, δ) will guide the prey position (optimal answer), and the other wolves (ω) will update their position relative to these wolves. First, the wolves will identify the prey, which is equivalent to the initial search in this algorithm; then, the wolves will surround the prey by updating their position and attack the prey, which is the local search [34-36]. First, the prey will be surrounded by the gray wolf, and the distance between the prey position and the gray wolf is shown by Eq. (11).

$$\vec{D} = |\vec{C} \cdot \vec{X}_p(t) - \vec{X}(t)| \tag{11}$$

In Eq. (11), $\vec{C}$: coefficient vector, $\vec{X}_p(t)$: prey position, $\vec{X}(t)$: gray wolf position. In Eq. (12), represents how the wolf moves towards the prey, and in which the wolf moves towards the new position.

$$\vec{X}(t+1) = \vec{X}_p(t) - \vec{A} \cdot \vec{D} \tag{12}$$

In Eq. (12), $\vec{A}$ is the coefficient vector and $\vec{X}(t+1)$ is the new position of the gray wolf. The coefficient vector $\vec{C}$will be calculated by Eq. (13).

$$\vec{C} = 2 \cdot \vec{r}_2 \tag{13}$$

where $\vec{r}_2$ is a random vector in the interval [0,1]. The coefficient vector $\vec{A}$ is also represented by Eq. (14).

$$\vec{A} = 2\vec{a} \cdot \vec{r}_1 - \vec{a} \tag{14}$$

In Eq. (14), $\vec{r}_2$ is a random vector in [0,1], and $\vec{a}$ decreases linearly from 2 to 0 during the iterations, as described in Eq. (15).

$$a = 2 - t \cdot \frac{2}{MaxIter} \tag{15}$$

Eq. (15) defines MaxIter as the maximum number of iterations. Since the optimal prey position is unknown, it is assumed that the top three wolves (α, β, δ) have the best knowledge. Their distances are obtained using Eqs. (16), (17), and (18).

$$\vec{D}_\alpha = \left|\vec{C}_1 \cdot \vec{X}_\alpha - \vec{X}\right| \tag{16}$$

$$\vec{D}_\beta = \left|\vec{C}_2 \cdot \vec{X}_\beta - \vec{X}\right| \tag{17}$$

$$\vec{D}_\delta = \left|\vec{C}_3 \cdot \vec{X}_\delta - \vec{X}\right| \tag{18}$$

In Eqs. (16), (17), and (18), $\vec{D}_\alpha$:distance from wolf α, $\vec{D}_\beta$:distance from wolf β, $\vec{D}_\delta$:distance from wolf δ. $\vec{X}_\alpha$: position of wolf α, $\vec{X}_\beta$:position of wolf β and $\vec{X}_\delta$ is the position of wolf δ. The vectors $\vec{C}_1$, $\vec{C}_2$, and $\vec{C}_3$ are calculated independently for each of the leader wolves via Eq. (13). The temporary proposed position for the current wolf to move towards wolf α is obtained via Eq. (19) (best solution). The temporary proposed position for the current wolf to move towards wolf β is obtained via Eq. (20) (second solution). The temporary proposed position for the current wolf's movement towards wolf δ is obtained through Eq. (21) (third solution) [34-36].

$$\vec{X}_1 = \vec{X}_\alpha - \vec{A}_1 \cdot \vec{D}_\alpha \tag{19}$$

$$\vec{X}_2 = \vec{X}_\beta - \vec{A}_2 \cdot \vec{D}_\beta \tag{20}$$

$$\vec{X}_3 = \vec{X}_\delta - \vec{A}_3 \cdot \vec{D}_\delta \tag{21}$$

In Eqs (19), (20), and (21), the vectors $\vec{A}_1$, $\vec{A}_2$, and $\vec{A}_3$ are calculated independently for each of the leader wolves through Eq. (14). Finally, the position of the new wolf will be obtained through Eq. (22).

$$\vec{X}(t+1) = \frac{\vec{X}_1 + \vec{X}_2 + \vec{X}_3}{3} \tag{22}$$

In order to ensure the effective and robust performance of the PD-PI cascaded controller against disturbances and changes in the parameters of the DDBC, the GWO algorithm has been used. In this paper, the objective function in optimizing the parameters of the PD-PI cascaded controller has been obtained based on Eq. (23). The objective function is a combination of the overshoot and settling time, and by minimizing it by the GWO algorithm, the PD-PI cascaded controller will lead to a fast response without overshoot.

$$\min \text{Objective Function} = (1-\rho)\times m + \rho \times t \tag{23}$$

In Eq. (23), m is the maximum overshoot percentage and t is the settling time (defined within a 2% tolerance band). The parameter ρ, which can range from 0 to 1, allows the designer to give greater weight to either the overshoot or the settling time based on specific requirements. For this study, following extensive testing over values from 0.1 to 0.99, ρ was empirically set to 0.95. The optimization constraints in Eq. (24) show that the allowable range for the PD-PI cascaded controller parameters is shown.

$$\begin{aligned} 0.001 \le K_P \le 3 \\ 0.001 \le K_D \le 3 \\ 0.001 \le K_{P1} \le 3 \\ 0.001 \le K_I \le 3 \end{aligned} \tag{24}$$

The flowchart of the adjustment of the parameters of the PD-PI cascaded controller used in the DDBC by the GWO algorithm is shown in Figure 3. In Figure 4, the control structure of the proposed method (PD-PI(GWO)) for voltage regulation in the DDBC is shown.

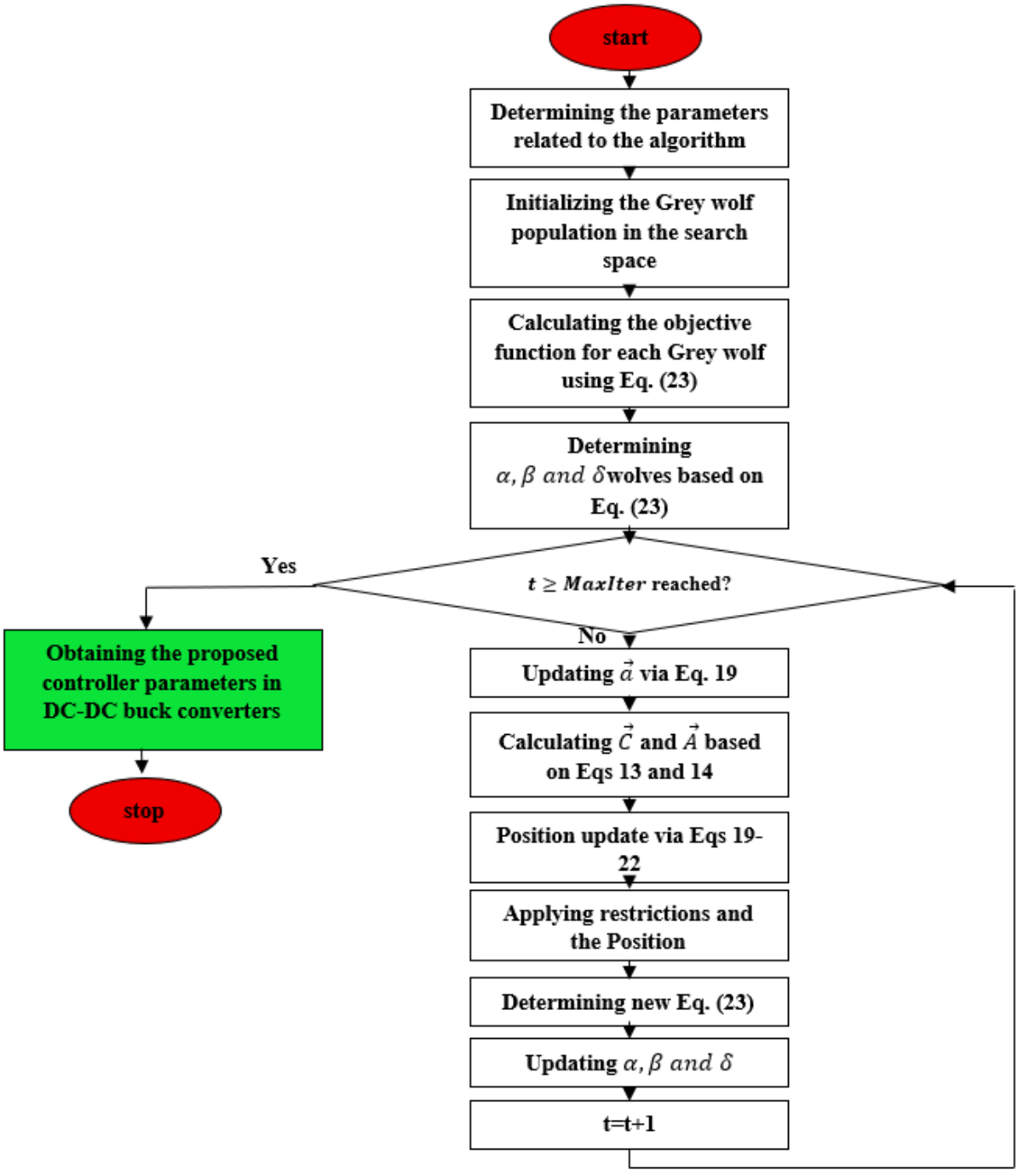

Figure 3. The flowchart of the adjustment of the parameters of the PD-PI cascaded controller used in the DDBC by the GWO algorithm

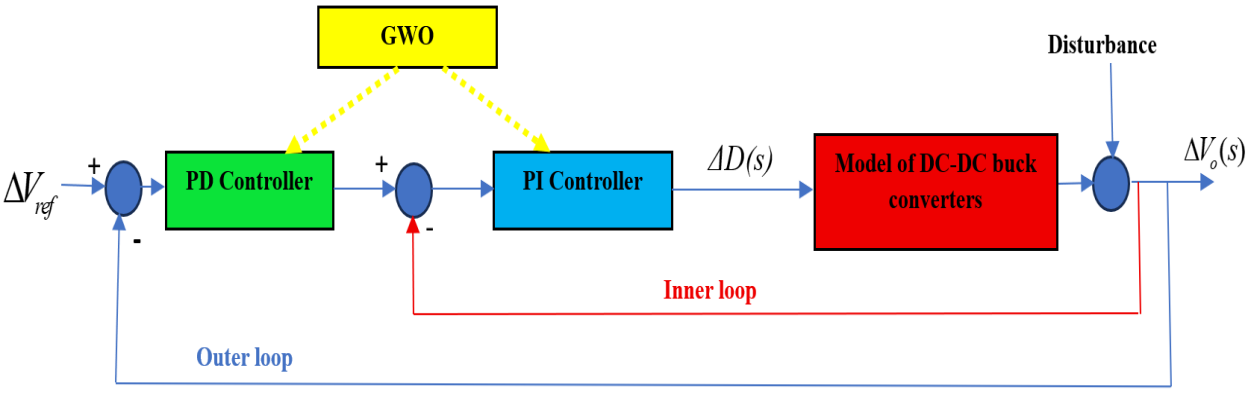

Figure 4. the control structure of the proposed method (PD-PI(GWO)) for voltage regulation in the DDBC

In Table (2), the parameters related to the Gray Wolf algorithm for adjusting the PD-PI cascaded control parameters are shown.

Table (2), the parameters related to the Gray Wolf algorithm for adjusting the PD-PI cascaded control parameters

parameter	value
Number of wolves (N)	50
Number of iterations (T_{max})	50
a	2 →0
$\vec{r}_1, \vec{r}_2$	[0,1]
$\vec{C}$	[0,2]

4-Simulation:

Simulation has been performed in three scenarios to compare the proposed method (PD-PI(GWO)) with other control methods (PD-PI(EEFO) and PD-PI(FLA)). Scenario 1 evaluates the proposed approach against alternative control strategies for voltage tracking in the DDBC. Scenario 2 assesses the proposed method against alternative control techniques for DDBC voltage tracking under parameter variations. In scenario (3), the proposed method is compared with other control methods in DDBC voltage tracking, considering the effect of disturbance.

4-1-Scenario (1):

To identify the most effective optimization strategy, the performance of FLA, EEFO, and GWO

10.22060/EEJ.2026.25791.6005

algorithms was initially evaluated based on the objective function defined in Eq. (23). In this scenario, first, the reference voltage of the DDBC has been changed in a stepwise manner according to Figure 5. In Figure 6, the convergence of the proposed algorithm considering the objective function according to Eq. (23) with the FLA and EEFO algorithms is shown. In Table 3, the comparison of different algorithms considering criteria such as the objective function (Eq. 23), IAE, ITAE, ISE, and ITSE has been discussed. According to Table 3, the GWO algorithm has the best performance in minimizing the objective function (Eq. (23)) compared to other algorithms, and its value is 3.26×10^{-9}. Also, the proposed algorithm (GWO) has the best performance in terms of four criteria, IAE, ITAE, ISE, and ITSE, compared to other algorithms. Table 4 shows the optimal values of the cascaded controller parameters (PD-PI using the GWO algorithm. The closed-loop Bode plot of the frequency response of the converter from the voltage reference to the output voltage based on different control methods is shown in Figure 7. This plot is a measure of the bandwidth, resonant peak (indicating damping), and closed-loop frequency behavior. The Bode diagram analysis was performed based on various control methods as shown in Table (5). The closed-loop Bode diagram shows that the proposed controller (PD-PI(GWO)) provides the best performance in the frequency domain (and consequently time domain) with the highest bandwidth and lowest resonance peak. This controller provides an optimal balance between tracking speed, oscillation damping, and stability. Figure 8 shows the output voltage in the DDBC based on three different control methods (PD-PI(EEFO), PD-PI(GWO), and PD-PI(FLA)). Table (6) provides a general comparison of the proposed control method (PD-PI(GWO)) with other control methods (PD-PI(EEFO), PD-PI(FLA)) in terms of various criteria such as ST, t_{rise}, O_s, t_{peak}, and ess. According to Table (6), the proposed method and other control methods have zero overshoot (Os), but in terms of the other four criteria, namely ST, t_{rise}, t_{peak}, and e_{ss}, the proposed method performs better than other control methods.

10.22060/EEJ.2026.25791.6005

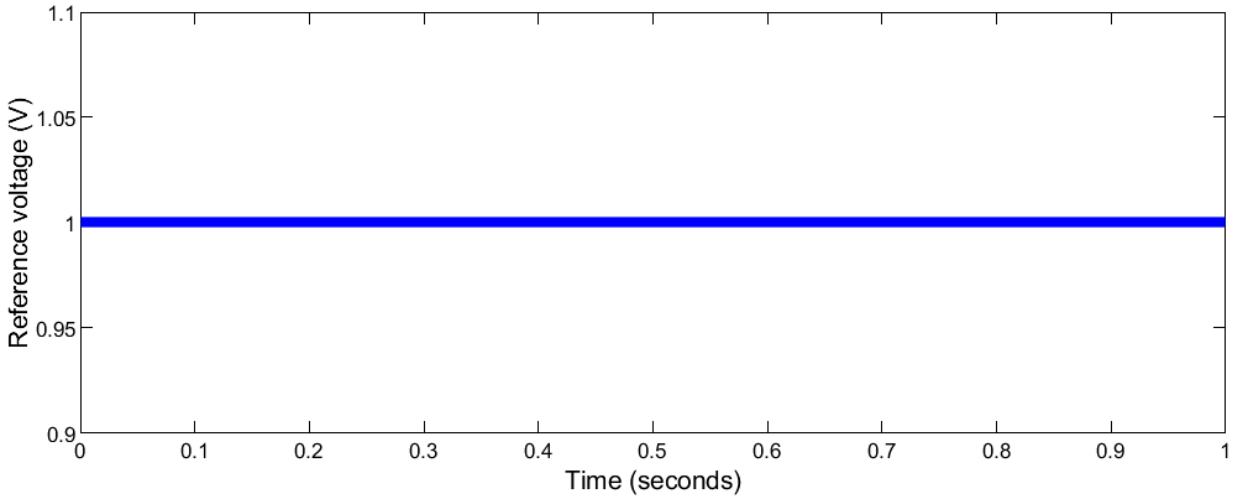

Figure 5. The reference voltage of the DDBC

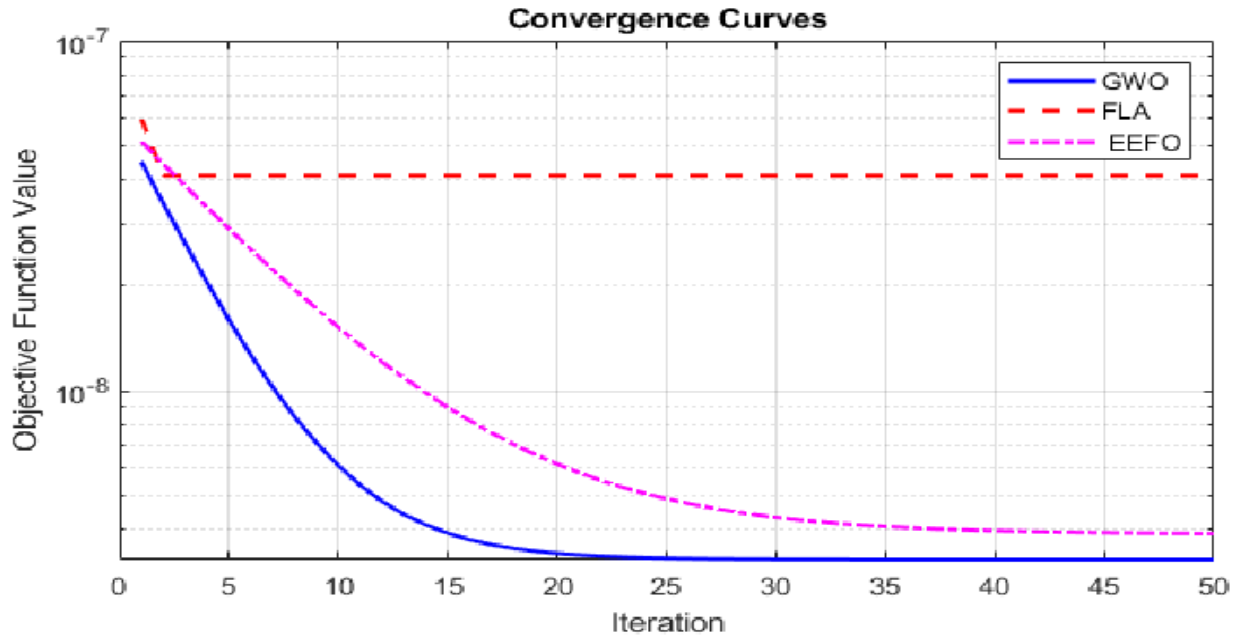

Figure 6, the convergence of the proposed algorithm considering the objective function according to Eq. (23) with the FLA and EEFO algorithms

Table 3. The comparison of different algorithms considering criteria, Scenario (1)

method	J(Eq. 23)	IAE	ISE	ITAE	ITSE
PD-PI(GWO)	3.26×10^{-9}	1.1×10^{-8}	5.55×10^{-9}	1.2×10^{-15}	3.08×10^{-17}
PD-PI(EEFO)	3.28×10^{-9}	1.7×10^{-8}	8.39×10^{-9}	1.73×10^{-15}	7.04×10^{-17}
PD-PI(FLA)	4.1×10^{-8}	2×10^{-8}	9.92×10^{-9}	2.1×10^{-15}	9.86×10^{-17}

Table 4. The optimal values of the cascaded controller parameters (PD-PI using the GWO algorithm)

parameter	value

10.22060/EEJ.2026.25791.6005

K_P	0.5
K_D	0.5
K_{P1}	1
K_I	2

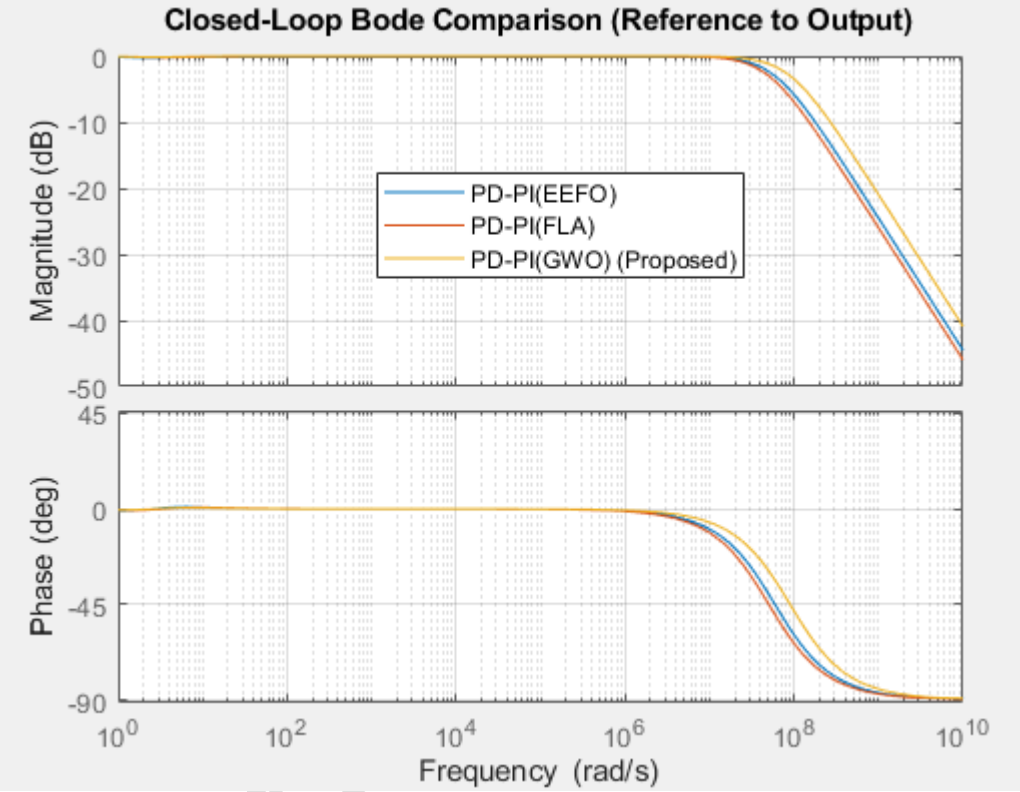

Figure 7: The closed-loop Bode plot of the frequency response of the converter from the voltage reference to the output voltage based on different control methods

Table (5): The Bode diagram analysis was performed based on various control methods

Characteristic	PD-PI(GWO)	PD-PI(EEFO)	PD-PI(FLA)
Resonant Peak (Magnitude overshoot)	Lowest	Moderate	Highest
Closed-Loop Bandwidth (Speed)	Highest	Moderate	Lowest
Damping (Oscillation suppression)	Best	Good	Acceptable
Response Speed	Fastest	Moderate	Slowest

Relative Stability (Robustness)	Excellent	Good	Acceptable

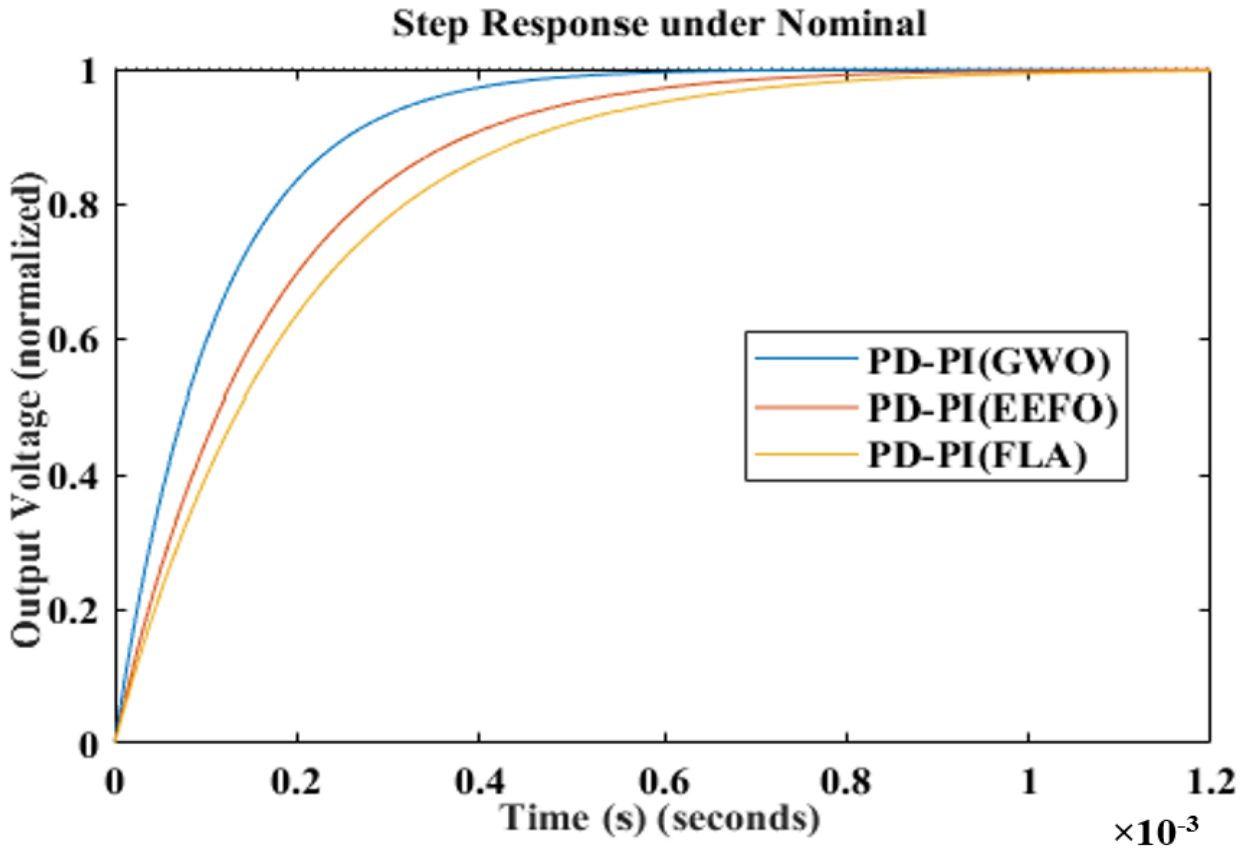

Figure 8. The output voltage in the DDBC based on three different control methods, Scenario (1)

Table (6). The general comparison of the proposed control method (PD-PI(GWO)) with other control methods (PD-PI(EEFO), PD-PI(FLA)), Scenario (1)

Method	ST(sec)	t_{rise}(sec)	Os(%)	t_{peak}(sec)	e_{ss}(%)
PD-PI(GWO)	4.34×10^{-4}	2.44×10^{-4}	0	8.13×10^{-5}	0.0027
PD-PI(EEFO)	6.56×10^{-4}	3.68×10^{-4}	0	3.30×10^{-4}	0.0030
PD-PI(FLA)	7.77×10^{-4}	4.36×10^{-4}	0	3.84×10^{-4}	0.0035

4-2-Scenario (2):

In scenario (2), the proposed method is compared with other control methods in tracking the voltage of the DDBC by considering the change of parameters. In this scenario, first, the reference voltage of the DDBC is changed in a stepwise manner as shown in Figure 5. In Figure 9, the output voltage in the DDBC is shown based on three control methods (PD-PI(EEFO), PD-PI(GWO), and PD-PI(FLA)) and by considering the change of parameters in the capacitor capacity (C=+10%). In Figure 10, the output voltage in the DDBC is shown based on three control methods (PD-

PI(EEFO), PD-PI(GWO), and PD-PI(FLA)) and by considering the change of parameters in the capacitor capacity (C=-10%). In Figure (11), the output voltage in the buck converter is shown based on three control methods (PD-PI(EEFO), PD-PI(GWO), and PD-PI(FLA)) and considering the change in the parameters in the inductor capacitance (L=+15%). In Figure (12), the output voltage in the DDBC is shown based on three control methods (PD-PI(EEFO), PD-PI(GWO), and PD-PI(FLA)) and considering the change in the parameters in the inductor capacitance (L=-15%). In Table (7), the overall comparison of the proposed control method (PD-PI(GWO)) with other control methods (PD-PI(EEFO), PD-PI(FLA)) in terms of various criteria such as ST, t_{rise}, Os, t_{peak}, ess, and also considering the effect of changing various parameters is discussed. According to Table (7), the proposed method has performed well and has been able to outperform other control methods in terms of various criteria (ST, t_{rise}, Os, t_{peak}, e_{ss}), and the results of this scenario indicate that the proposed PD-PI(GWO) method has been able to perform robustly against changes in parameters related to the DDBC.

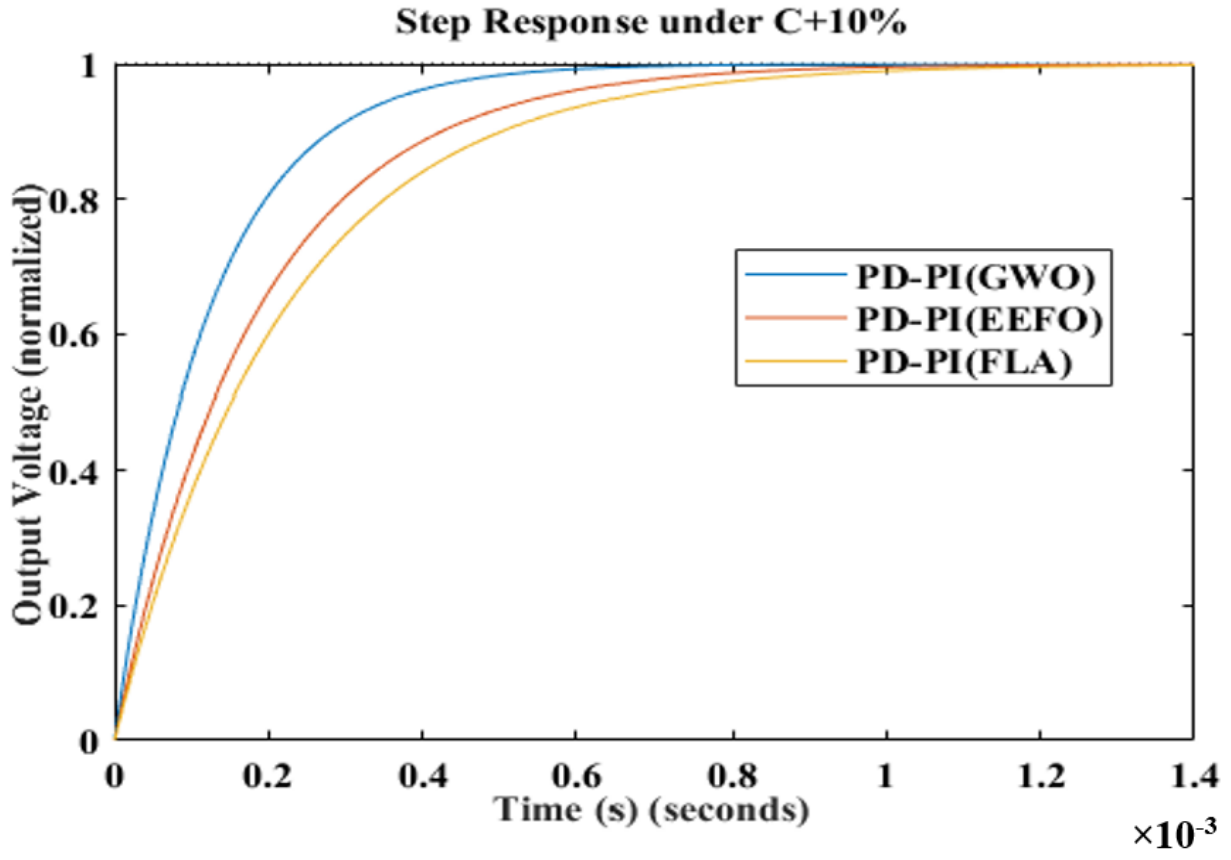

Figure 9. The output voltage of the DDBC based on three different control methods, considering the uncertainty in C=+10%.

10.22060/EEJ.2026.25791.6005

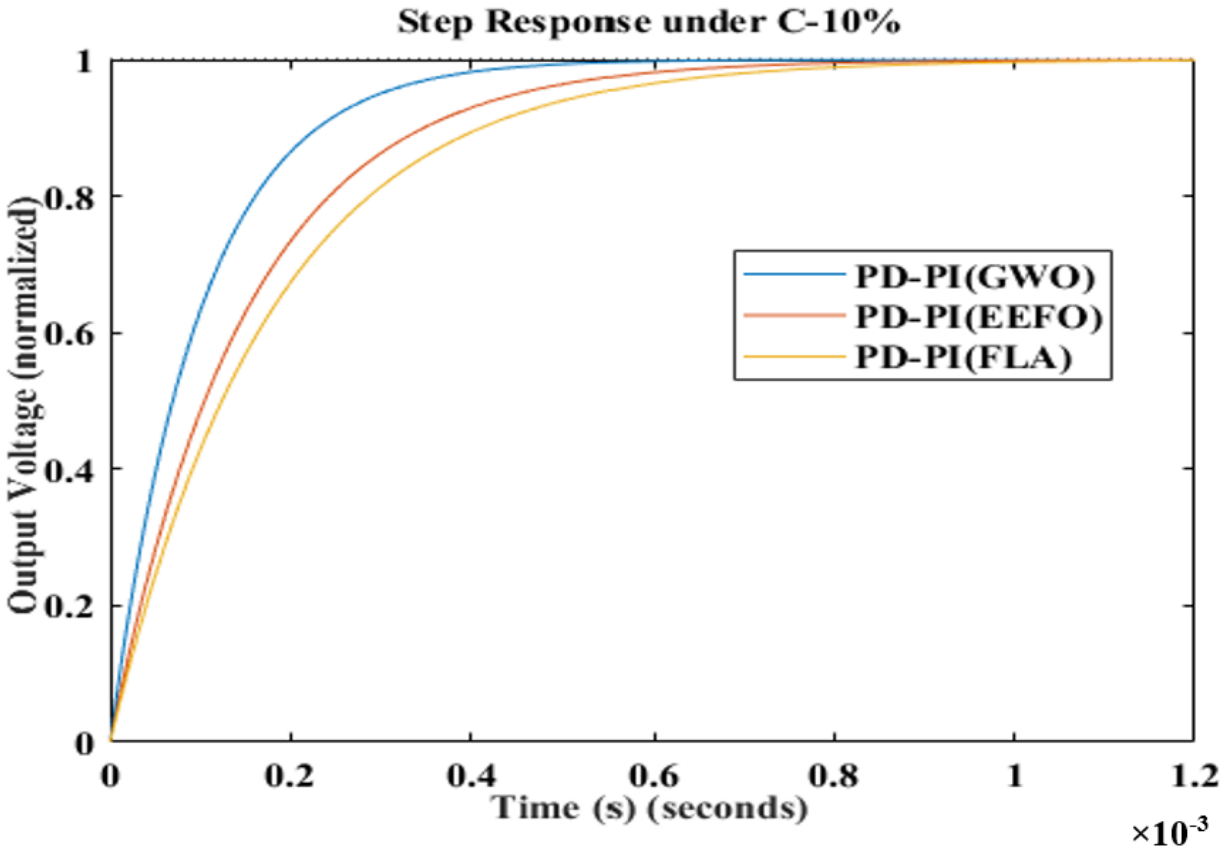

Figure 10. The output voltage of the DDBC based on three different control methods, considering the uncertainty in C=-10%.

10.22060/EEJ.2026.25791.6005

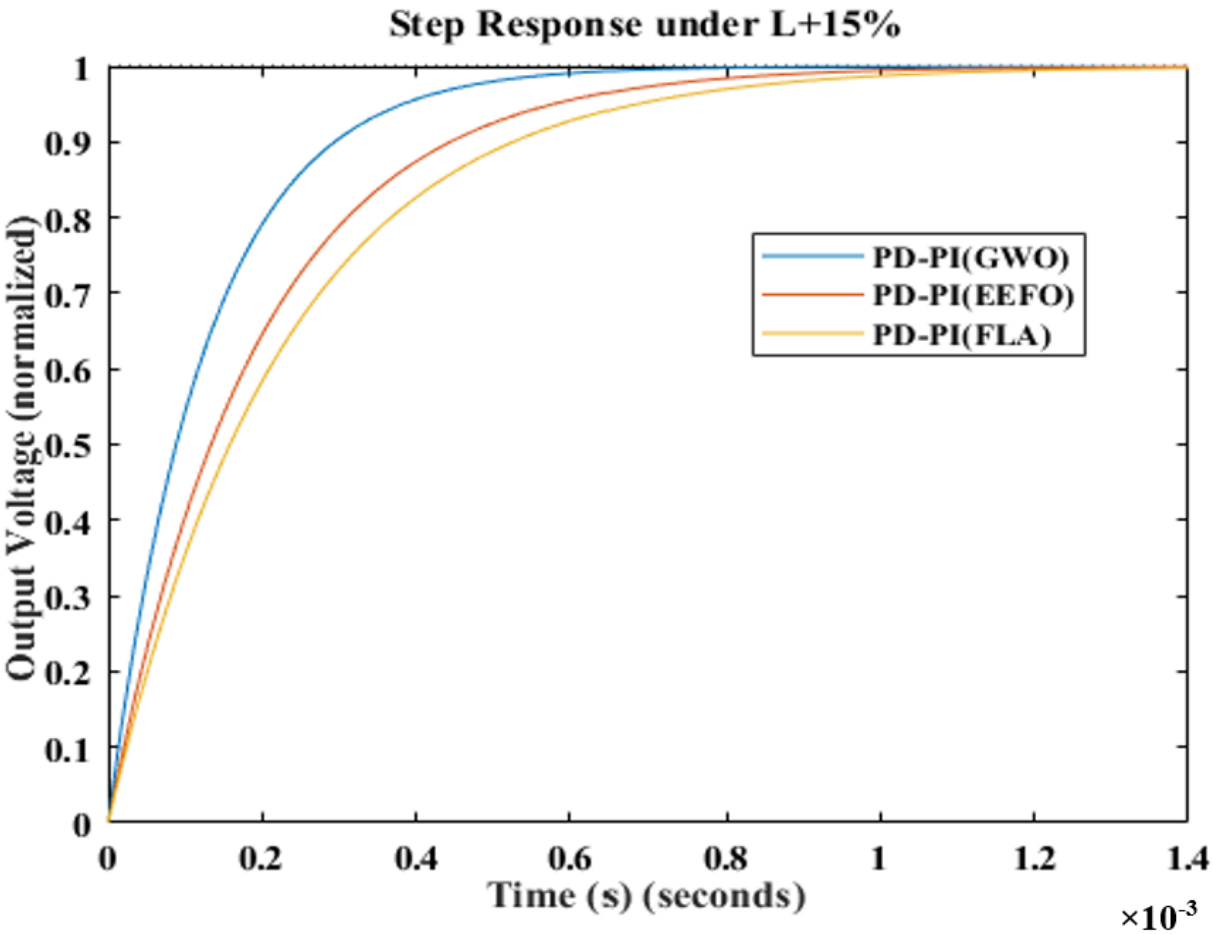

Figure 11. The output voltage of the DDBC based on three different control methods, considering the uncertainty in L=+15%

10.22060/EEJ.2026.25791.6005

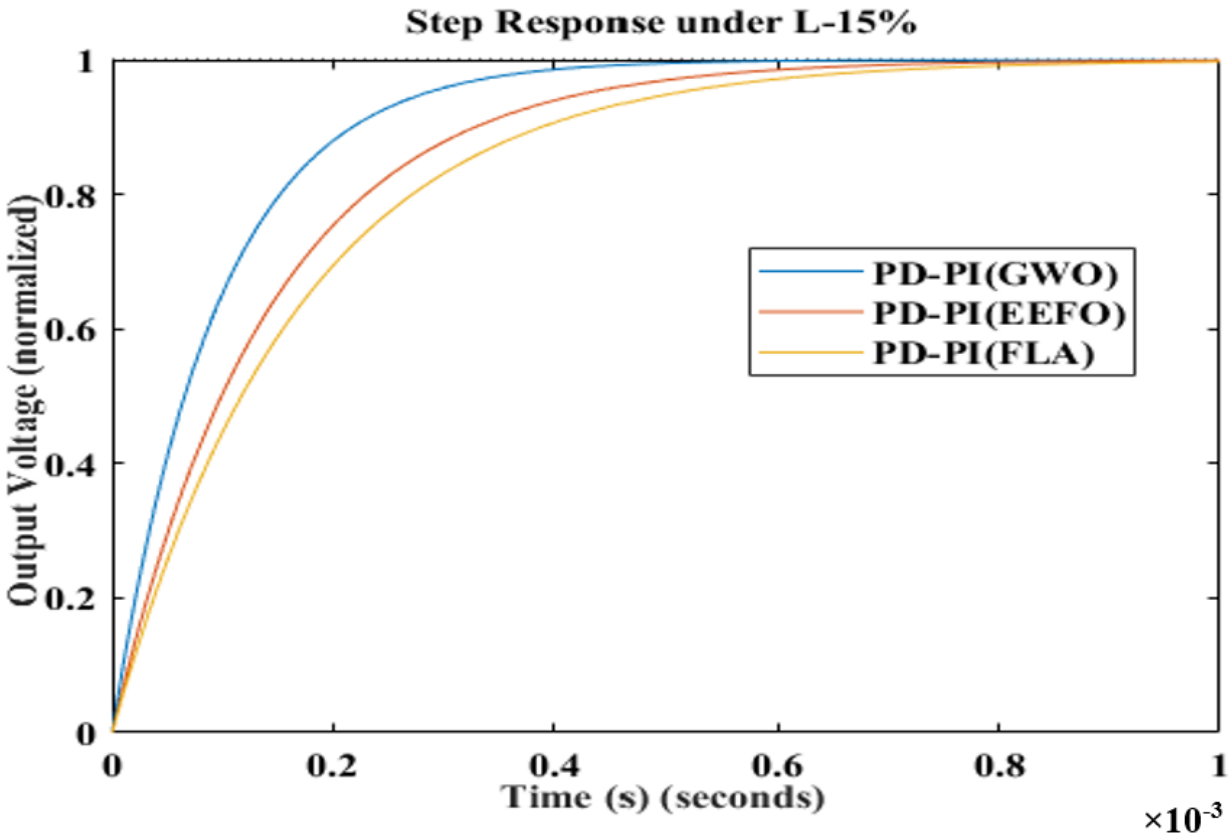

Figure 12. The output voltage of the DDBC based on three different control methods, considering the uncertainty in L=-15%

Table (7). The general comparison of the proposed control method (PD-PI(GWO)) with other control methods (PD-PI(EEFO), PD-PI(FLA)), Scenario (2)

Method	ST(sec)	t_{rise}(sec)	Os(%)	t_{peak}(sec)	e_{ss}(%)
PD-PI(GWO)(C=+10%)	4.78×10^{-4}	2.68×10^{-4}	0	8.94×10^{-5}	0.0027
PD-PI(GWO)(C=-10%)	3.91×10^{-4}	2.19×10^{-4}	0	7.32×10^{-5}	0.0027
PD-PI(GWO)(L=+15%)	5×10^{-4}	2.80×10^{-4}	0	9.35×10^{-5}	0.0027
PD-PI(GWO)(L=-15%)	3.69×10^{-4}	2.07×10^{-4}	0	6.91×10^{-5}	0.0028
PD-PI(EEFO)(C=+10%)	7.22×10^{-4}	4.05×10^{-4}	0	2.83×10^{-4}	0.0030
PD-PI(EEFO)(C=-10%)	5.91×10^{-4}	3.31×10^{-4}	0	3.77×10^{-4}	0.0030
PD-PI(EEFO)(L=+15%)	7.55×10^{-4}	4.24×10^{-4}	0	2.99×10^{-4}	0.0030
PD-PI(EEFO)(L=-15%)	5.58×10^{-4}	3.13×10^{-4}	0	3.62×10^{-4}	0.0032
PD-PI(FLA)(C=+10%)	8.54×10^{-4}	4.79×10^{-4}	0	3.84×10^{-4}	0.0035
PD-PI(FLA)(C=-10%)	6.99×10^{-4}	3.92×10^{-4}	0	4.22×10^{-4}	0.0035
PD-PI(FLA)(L=+15%)	8.93×10^{-4}	5.01×10^{-4}	0	3.72×10^{-4}	0.0038
PD-PI(FLA)(L=-15%)	6.60×10^{-4}	3.70×10^{-4}	0	4.08×10^{-4}	0.0038

4-3-Scenario (3):

10.22060/EEJ.2026.25791.6005

This scenario evaluates the proposed technique against other control strategies for DDBC voltage tracking while accounting for the impact of disturbances. Disturbance is applied to the DDBC as shown in Figure (13). In Figures (14) and (15), the output voltage in the DDBC is shown based on three control methods (PD-PI(EEFO), PD-PI(GWO) and PD-PI(FLA))) and considering the effect of disturbance. In Table (8), the three control methods (PD-PI(EEFO), PD-PI(GWO) and PD-PI(FLA))) are compared with each other based on the criteria of maximum deviations and recovery time. According to Table (8), the proposed method (PD-PI(GWO)) has a value of -2.0002v in terms of the criterion of maximum deviations, which is the lowest value among the control methods. Also, in terms of recovery time, the proposed method has a value of 2.38×10^{-8}, which in terms of this criterion also performs better than other control methods.

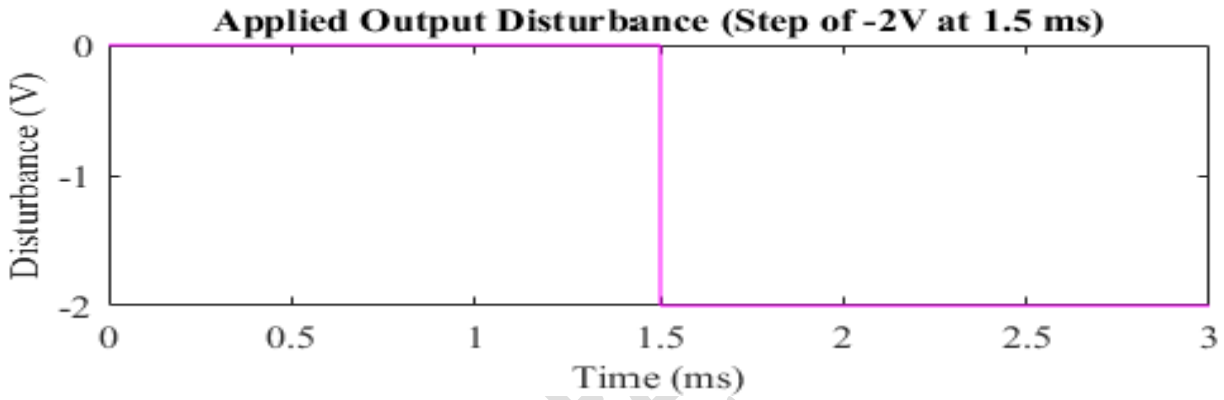

Figure 13. Applied disturbance Output to the DDBC

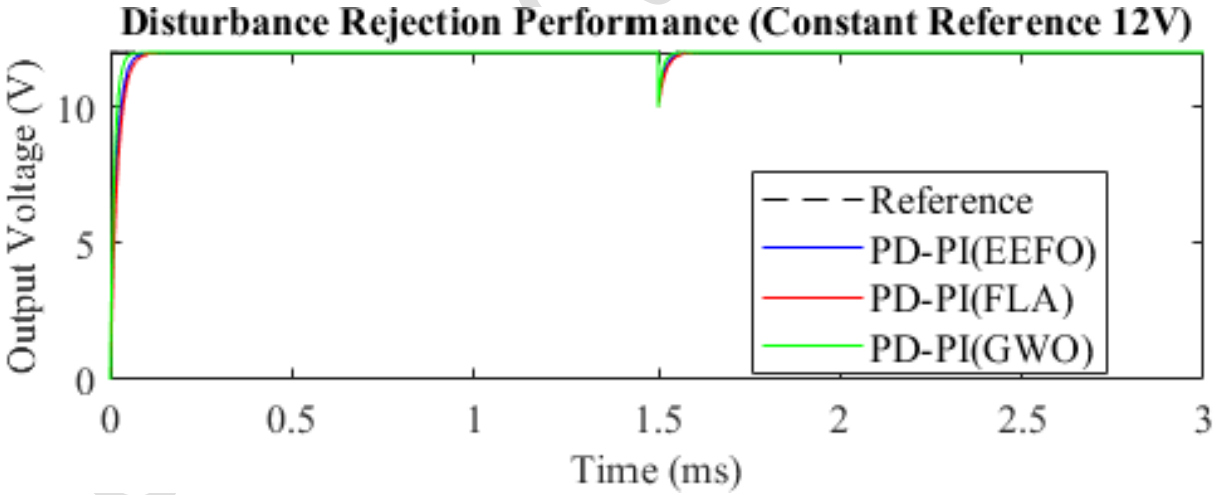

Figure 14. The output voltage in the DDBC based on three different control methods, Scenario (3)

10.22060/EEJ.2026.25791.6005

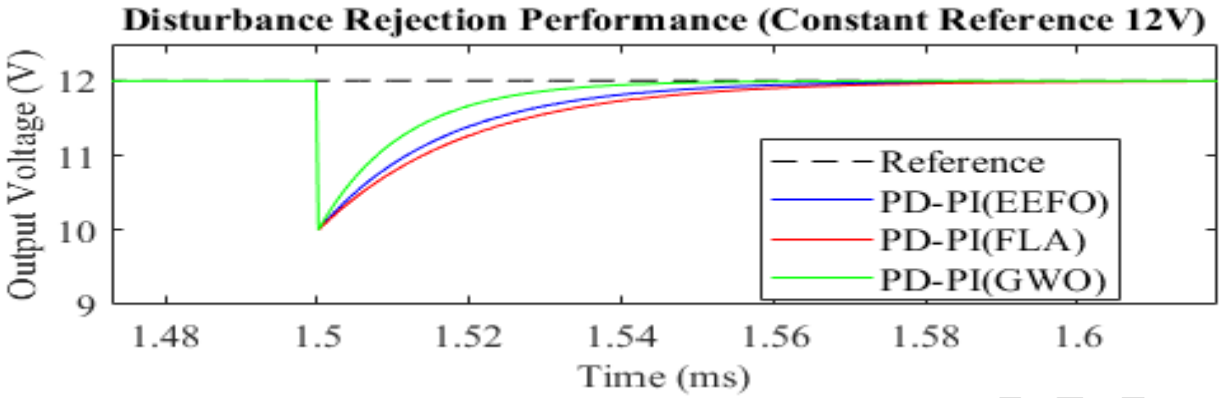

Figure 15. The output voltage in the DDBC based on three different control methods, Scenario (3)

Table (8). The general comparison of the proposed control method (PD-PI(GWO)) with other control methods (PD-PI(EEFO), PD-PI(FLA)), Scenario (3)

Method	Max Deviation (V)	Recovery Time (s)
PD-PI(GWO)	-2.0002v	2.38×10^{-4}
PD-PI(EEFO)	-2.0003v	3.58×10^{-4}
PD-PI(FLA)	-2.0004v	4.24×10^{-4}

5- Conclusion:

This paper investigates the output voltage control of a DDBC, treated as a nonlinear system susceptible to disturbances and parametric uncertainties. To achieve a fast dynamic response, effective damping of voltage fluctuations, and the elimination of steady-state error, a cascaded PD-PI control architecture is proposed. In this configuration, the outer-loop of the PD controller manages fast voltage response and damping the fluctuations, while the inner-loop of the PI controller eliminates the steady-state errors arising from reference voltage variations or load disturbances. To ensure precise and optimal tuning of the internal parameters, the Grey Wolf Optimizer (GWO) is employed. Due to its intelligent search capabilities, minimal parameter sensitivity, also stable and convergence, the GWO facilitates optimal performance. The efficiency of the proposed PD-PI(GWO) method is validated through comparative analyses against several control scenarios, including PD-PI(EEFO) and PD-PI(FLA), under disturbances and changes in various parameters. The simulation results demonstrate significant improvements in performance metrics:

- Settling time improvement related to voltage deviations in the DDBC by 33%
- Rise time improvement related to the DDBC voltage by 34%
- Peak time improvement related to the DDBC voltage by 94%
- Steady state error improvement related to the DDBC voltage deviation by 10%

Reference:

[1] Chhab, N., Abouloifa, A., Elbouchikhi, E., Houari, A., & Lachkar, I. (2026). ADRC-based dual-loop control and stability analysis of stacked interleaved DC–DC buck converter for hydrogen production using PEM electrolyzer. Energy Reports, 15, 109154.
[2] Shahbazi, M., & Amiri, F. (2019, December). Designing a Neuro-Fuzzy controller with CRPSO and RLSE algorithms to control voltage and frequency in an isolated microgrid. In 2019 international power system conference (PSC) (pp. 588-594). IEEE.
[3] Amiri, F., & Moradi, M. H. (2023). Design of a new control method for dynamic control of the two-area microgrid: F. Amiri and MH Moradi. Soft Computing, 27(10), 6727-6747.
[4] Demirel, O. (2026). Current Estimator LESO-Based Discrete-Time LADRC of a DC-DC Buck Converter. Electronics, 15(5), 1133.
[5] Dutta, J., Das, R., & Yadav, A. (2026). PI controller design for non-ideal DC-DC buck converter using grey wolf optimization algorithm. International Journal of Information Technology, 1-13.
[6] Cao, K., Gu, J., Chen, D., Li, J., Li, P., & Li, S. (2026). Fractional-order reduced-order extended state observer-based controller for DC-DC buck converter with time delay estimation. Physica Scripta, 101(5), 055206.
[7] Hinov, N., Kabakchieva, R., & Stanchev, P. (2026). A Fuzzy Satisfaction-Based Intelligent Framework for Multiobjective Design of a Buck DC-DC Converter Under Uncertain Operating Conditions. Mathematics, 14(7), 1115.
[8] Jabari, M., Izci, D., Ekinci, S., Bajaj, M., & Zaitsev, I. (2024). Performance analysis of DC-DC Buck converter with innovative multi-stage PIDn (1+ PD) controller using GEO algorithm. Scientific Reports, 14(1), 25612.
[9] Nanyan, N. F., Ahmad, M. A., & Hekimoğlu, B. (2024). Optimal PID controller for the DC-DC buck converter using the improved sine cosine algorithm. Results in Control and Optimization, 14, 100352.
[10] Sorouri, H., Sedighizadeh, M., Oshnoei, A., & Khezri, R. (2022). An intelligent adaptive control of DC–DC power buck converters. International Journal of Electrical Power & Energy Systems, 141, 108099.

[11] Hanif, M. I. F. M., Suid, M. H., & Ahmad, M. A. (2019). A piecewise affine PI controller for buck converter generated DC motor. *Int. J. Power Electron. Drive Syst*, *10*(3), 1419.

[12] Chincholkar, S., Tariq, M., Poshtan, M., & Sharaf, M. (2024). Normalized error-based PI controller and its application to the DC–DC buck converter. *Mathematics*, *12*(2), 240.

[13] Aguilar-Ibanez, C., Moreno-Valenzuela, J., García-Alarcón, O., Martinez-Lopez, M., Acosta, J. Á., & Suarez-Castanon, M. S. (2021). PI-type controllers and Σ–Δ modulation for saturated DC-DC buck power converters. *IEEE Access*, *9*, 20346-20357.

[14] Dinniyah, F. S., Wahab, W., & Alif, M. (2017). Simulation of buck-boost converter for solar panels using PID controller. *Energy Procedia*, *115*, 102-113.

[15] Samosir, A. S., Sutikno, T., & Mardiyah, L. (2023). Simple formula for designing the PID controller of a DC-DC buck converter. *International Journal of Power Electronics and Drive Systems*, *14*(1), 327-336.

[16] Nishat, M. M., Faisal, F., Evan, A. J., Rahaman, M. M., Sifat, M. S., & Rabbi, H. F. (2020). Development of genetic algorithm (ga) based optimized PID controller for stability analysis of DC-DC buck converter. *Journal of Power and Energy Engineering*, *8*(09), 8.

[17] Hekimoğlu, B., & Ekinci, S. (2020). Optimally designed PID controller for a DC-DC buck converter via a hybrid whale optimization algorithm with simulated annealing. *Electrica*, *20*(1), 19-27.

[18] Rajamani, M. P. E., Rajesh, R., & Willjuice Iruthayarajan, M. (2023). Design and experimental validation of PID controller for buck converter: A multi-objective evolutionary algorithms based approach. *IETE Journal of Research*, *69*(1), 21-32.

[19] Adhul, S. V., & Ananthan, T. (2020). FOPID controller for buck converter. *Procedia computer science*, *171*, 576-582.

[20] Ghamari, S. M., Molaee, H., Ghahramani, M., Habibi, D., & Aziz, A. (2025). Design of an improved robust fractional-order PID controller for buck–boost converter using snake optimization algorithm. *IET Control Theory & Applications*, *19*(1), e70008.

[21] Isen, E. (2022). Determination of different types of controller parameters using metaheuristic optimization algorithms for buck converter systems. *IEEE Access*, *10*, 127984-127995.

[22] Aseem, K., & Selva Kumar, S. (2022). Hybrid k-means Grasshopper Optimization Algorithm based FOPID controller with feed forward DC–DC converter for solar-wind generating system. *Journal of Ambient Intelligence and Humanized Computing*, *13*(5), 2439-2462.

[23] Saleem, O., Ahmad, K. R., & Iqbal, J. (2024). Fuzzy-augmented model reference adaptive PID control law design for robust voltage regulation in DC–DC buck converters. *Mathematics*, *12*(12), 1893.

[24] Campos, M. W. D. S., Prado, E. M., De Medeiros, R. L., Fantesia, M. P., De Oliveira, W. D., Conceição, V. C., ... & Ayres, F. A. D. C. (2025). Development of a Hybrid Fractional-Order Fuzzy-PID Controller Applied to a DC-DC Buck Converter. *IEEE Transactions on Circuits and Systems II: Express Briefs*.

[25] Nejad, M. B., Ghamari, S. M., & Mollaee, H. (2023). Adaptive neuro-fuzzy inference systems controller design on Buck converter. *The Journal of Engineering*, *2023*(10), e12316.

[26] Ertekin, D., & Özden, M. (2026). Adaptive neuro fuzzy control of a high gain bidirectional power converter for photovoltaic-hydrogen renewable electric vehicles with enhanced lifespan and reliability. *AEU-International Journal of Electronics and Communications*, 156198.

[27] Garcés-Ruiz, A., Gil-González, W., & Montoya, O. D. (2024). Stability analysis for an ad-hoc model predictive control in DC/DC converters with a constant power load. *Results in Engineering*, *22*, 102262.

[28] Pyarilal, A., Vellukkeel, S., & Bepinkumar, B. (2025). Design and Prototyping of a Thermoelectric Emulator Using an MPC-Controlled Buck Converter for I–V Curve Generation. *IEEE Transactions on Industrial Electronics*.

[29] Ullah, Q., Busarello, T. D. C., Brandao, D. I., & Simões, M. G. (2023). Design and performance evaluation of SMC-based DC–DC converters for microgrid applications. *Energies*, *16*(10), 4212.

[30] Acosta-Rodríguez, R. A., Martinez-Sarmiento, F. H., & Múñoz-Hernandez, G. A. (2025). Design methodology for optimized control of high-power quadratic buck converters using sliding mode and hybrid controllers. *IEEE Access*, *13*, 49416-49432.

[31] Izci, D., Ertuğrul, E., Ekinci, S., Jabari, M., Bajaj, M., Blazek, V., ... & Çelik, E. (2026). A novel EEFO-tuned cascaded PI–PD controller for nonlinear dynamic regulation of DC–DC buck converters under uncertainty. *Measurement and Control*, 00202940261424677.

[32] Amiri, F., & Moradi, M. H. (2023). Improvement of Frequency stability in the power system considering wind turbine and time delay. Journal of Renewable Energy and Environment, 10(1), 9-18.

[33] Amiri, F., & Moradi, M. H. (2025). Design of the PD-FOPID Controller Based on Rain Optimization Algorithm to Improve Virtual Inertia Control Performance in Islanded Microgrids. Iranian Journal of Electrical & Electronic Engineering, 21(1).

[34] Amrir, M. M. S., Ayid, Y. M., Elshewey, A. M., & Fouad, Y. (2026). A hybrid LSTM-GRU framework for lung cancer classification using GWO-WOA algorithm for hyperparameter tuning and BPSO for feature selection. *Scientific Reports*.

[35] Faris, H., Aljarah, I., Al-Betar, M. A., & Mirjalili, S. (2018). Grey wolf optimizer: a review of recent variants and applications. *Neural computing and applications*, *30*(2), 413-435.

[36] Negi, G., Kumar, A., Pant, S., & Ram, M. (2021). GWO: a review and applications. International journal of system assurance engineering and management, 12(1), 1-8.